Infinite Dilution Activity Coefficients for Trihexyltetradecyl Phosphonium Ionic Liquids: Measurements and COSMO-RS Prediction

Tamal Banerjee and Ashok Khanna*

Department of Chemical Engineering, Indian Institute of Technology, Kanpur, India

Separation of aliphatic and aromatic compounds was studied using the high molecular weight trihexyl-tetradecyl-phosphonium cation (thtd-Ph) based ionic liquids (ILs) with the anions chloride [Cl], tetrafluoroborate [BF_4], and bis(trifluoromethane sulfonylimide)[$(Tf)_2N$]. Infinite dilution activity coefficients (γ^∞) for these novel solvents have been measured at T = (308.15, 318.15, and 328.15) K, using gas−liquid chromatography. The aliphatic solutes studied were normal alkanes (pentane, hexane, heptane, octane), alkenes (hexene, heptene, octene), alkynes (hexyne, heptyne, octyne), cycloalkanes (cyclopentane, cylcohexane, cycloheptane), and alcohols (methanol, ethanol). The aromatic solute studied was benzene. The molar excess enthalpy at infinite dilution ($H^{E,\infty}$) was calculated using the temperature dependency of γ^∞ data. The selectivity values for the phosphonium-based ILs indicate a poorer separation capability than imidazolium- or pyridinium-based ILs. The values of γ^∞ have been found to be in the following order: alkanes > alkenes > alkynes > aromatics. Selectivity values indicate the IL [thtd-Ph][BF_4] as an effective solvent for the separation of benzene + alcohol systems. The γ^∞ measurements on the phosphonium ILs were further validated using the a priori COSMO-RS method. The COSMO-RS prediction was first benchmarked on the values obtained with [thtd-Ph] tris(pentafluoroethyl) trifluorophosphate, which gave the average absolute deviation (AAD) to be 15 %. Using COSMO-RS, γ^∞ values were obtained for the three phosphonium ILs, and the corresponding AADs were 9 %, 8 %, and 16 %.

Introduction

The study of ionic liquids (ILs) has become the subject of an increasing number of scientific investigations.[1,2] Activity coefficients at infinite dilution of a solute are used to quantify the volatility of the solute and to provide information about the intermolecular energy between solvent and solute. These are useful for the selection of solvents for extraction and extractive distillation. It allows the approximate calculation of the partition of the solute between the liquid and the vapor phase at low concentrations.

Since ILs have negligible vapor pressure, gas−liquid chromatography is the suitable method for measuring limiting activity coefficients of volatile solutes in ILs. The IL is used as the stationary phase. Most of the data till now have focused on the imidazolium based ILs.[3] Phosphonium salts are more thermally stable than the corresponding imidazolium salts. The imidazolium cation contains protons that are not entirely inert. They are acidic, which can result in carbene formation. Phosphonium salts, on the other hand, have no such acidic protons. Detailed properties of these ILs like densities, compressibities, etc. have been given recently by Esperanca et al.[4] Recently, Letcher and Reddy[5] have measured the γ^∞ for the phosphonium-based IL trihexyltetradecyl phosphonium trispentafluoroethyl trifluorophosphate [$(C_6H_{13})_3(C_{14}H_{29})$][$(C_2F_5)_3PF_3$].

In this work, infinite dilution activity coefficients have been measured for a series of hydrocarbons such as alkanes (pentane, hexane, heptane, octane), alkenes (1-hexene,1-heptene, 1-octene), alkynes (1-hexyne, 1-heptyne, 1-octyne), cycloparaffins (cyclopentane, cyclohexane, cycloheptane, cyclooctane), alcohols (methanol, ethanol), and benzene on the three ILs based on the trihexyl-tetradecyl-phosphonium (thtd-Ph) cation with the three anions chloride [Cl], tetrafluoroborate [BF_4], and bistrifluoromethanesulfonate imide [$(Tf)_2N$].

* Corresponding author. E-mail: akhanna@iitk.ac.in. Fax: +91-512-2590104.

Experimental Procedures

Chemicals. The ILs trihexyl(tetradecyl)-phosphonium chloride [thtd-Ph][Cl], trihexyl(tetradecyl)-phosphonium tetrafluoroborate [thtd-Ph][BF_4], and trihexyl(tetradecyl)-phosphonium trifluoromethanesulphonylimide [thtd-Ph][$(Tf)_2N$] were purchased from Fluka. The structures of all the three ILs are shown in Figure 1. The water content was reported by the supplier Fluka (Sigma Aldrich) to contain less than 100 ppm. Low-pressure vacuum was further applied for 24 h at 353 K to remove any traces of volatile contaminants including water. The organic solutes have been purchased from Alfa-Aesar, Lancaster, and were used without any further purification since the small amounts of impurities have a negligible effect on the retention times of the major peaks.

Procedure. The gas−liquid chromatography (GLC) has been performed on the NUCON 5700 gas chromatography apparatus. The columns used were of stainless steel of 1 m length and an internal diameter of 4 mm. The columns were washed, dried, and coiled prior to use. The support material used was of low surface area diatomaceous earth Chromosorb W-HP (100/120) mesh. Nitrogen carrier gas is passed to flush out any "fines" or broken particles generated due to the handling, storage, and transportation of the material. The purified IL samples were carefully weighed, dissolved in freshly distilled dichloromethane, and then quantitatively transferred to a preweighed amount of the support material. The mixture was then gently shaken, and vacuum-assisted rotary evaporation was used to remove the solvent. A heated stream of nitrogen gas was passed through the stationary phase for the final drying of the phase. To avoid possible residual adsorption effects of the solutes on the solid support, the amount of IL was about 30 mass % of the support material.

10.1021/je0602925 CCC: $33.50
Published on Web 10/06/2006

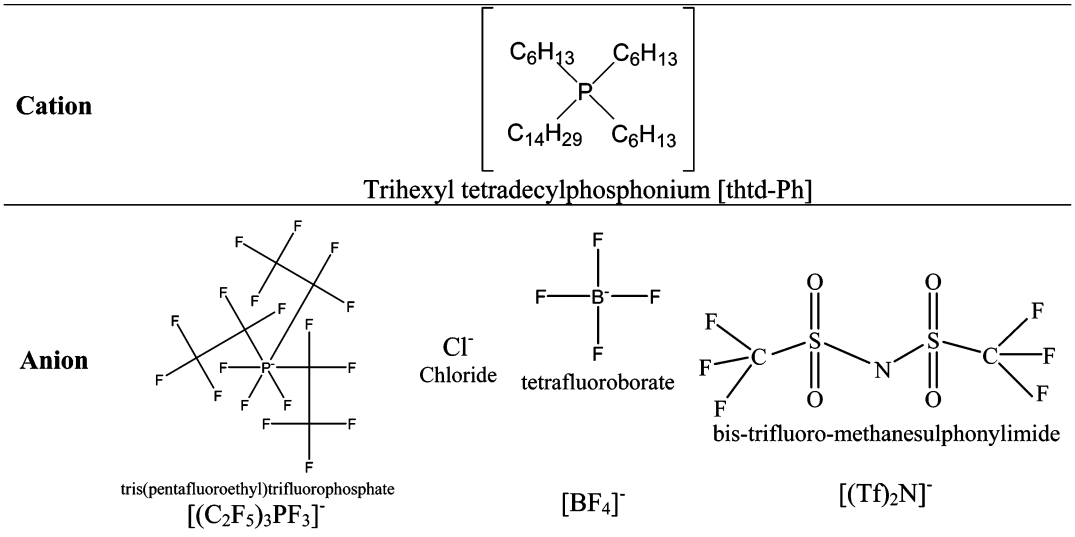

Figure 1. Structure of cations and anions used in this work.

A thermal conductivity detector (TCD) was used, the carrier gas being dry nitrogen. The carrier gas flow rate was determined using a calibrated soap bubble flowmeter, which had been placed at the outlet of the detector. The injection port was first heated; thereafter both the injection as well as detection temperatures were kept equal at 523 K. The flow rates, ranging from (20 to 30 mL·min^{-1}), had been set for a series of runs and were allowed to stabilize for at least 30 min before any γ_i^∞ measurements were made. Sample injections ranging from (0.1 to 0.5) μL were considered small enough to ensure the condition of infinite dilution of the solute on the column. Different volumes of each solute (i.e., (0.5 to 0.1) μL) along with the constant weight of stationary phase (0.0015 mol of IL) were initially tested in the column. We observed that there is no variation in retention time for different concentrations. Thus, we concluded that the state of infinite dilution had been realized to a high degree of approximation. Additionally, all the peaks were symmetrical in nature. A glass-walled U-tube manometer (i.d. 9 mm) was placed before the inlet of the column to determine the inlet column pressure. Outlet pressure was kept equal to atmospheric pressure. The pressure drop ($p_i - p_o$) was varied in the range (50.3 to 101.3) kPa, providing suitable retention times with sharp peaks. At a given temperature, each experiment was repeated at least twice to check the reproducibility. To check the stability of the experimental condition, such as the possible elution of the stationary phase by the nitrogen stream, measurements of retention time were repeated every 60 h for four selected solutes (hexane, hexene, cyclohexane, and benzene). No changes in the retention time were observed for the duration of 1 month.

A benchmarking system was conducted with the IL (1-hexyl-3-methylimidaozlium tetrafluoroborate) [HMIM][BF_4] as the stationary phase. The solutes here for which comparisons were made are alkanes (hexane, heptane, octane), alkenes (1-hexene, 1-heptene, 1-octene), alkynes (1-hexyne, 1-heptyne, 1-octyne), cycloparaffins (cyclohexane, cycloheptane), methanol, and benzene. The γ_i^∞ values obtained were within 6 % of that reported in the literature.[6] Long retention times and broad peaks were observed at lower temperatures, so no measurements were taken below 308.15 K. The temperature was controlled inside the column with a calibrated platinum resistance thermometer within ± 0.1 K.

Experimental Uncertainties. The measurements of retention time, column temperature, flow rate, input and output pressures, and mass of the stationary phase have experimental uncertainties. The value of the retention time lies between (5 and 25) min. The retention times were generally reproducible within (0.01 to 0.04) min. For the column temperature, the uncertainty was within ± 0.1 K. The flow rate was measured with an uncertainty of ± 0.1 cm^3·min^{-1}. The outlet pressure was measured with an uncertainty of ± 0.2 kPa. A reliable estimation for the mass of the stationary phase was quite difficult considering the fact that the amount of IL remaining on the walls of the rotating evaporator was difficult to measure. However, it should be noted that that the IL does not get lost in the evaporation process. The stationary phase was measured before and after the evaporation. The uncertainty in measuring the mass of the stationary phase was ± 0.0003 g. The overall uncertainty in measurement of γ^∞ calculated through error propagation law is ± 3 %.

Theory

The following equation according to Cruickshank et al.[7] was used to determine the infinite dilution activity coefficient:

$$\ln \gamma_{i,3}^\infty = \left(\frac{nRT}{V_N p_i^0}\right) - \frac{B_{ii} - V_i^0}{RT} p_i^0 + \frac{2B_{i2} - V_i^\infty}{RT} J p_o \qquad (1)$$

where $\gamma_{i,3}^\infty$ is the activity coefficient of solute i at infinite dilution, n is the number of moles of stationary component (0.0015 mol) (i.e., IL; with subscript 3) in the column, and V_N is the standardized retention volume. V_i^0 is the saturated molar volume of the solute i at temperature T, and V_i^∞ is the partial molar volume of the solute i in the solvent at infinite dilution. In the calculation V_i^0 is taken equal to V_i^∞. p_i^0 is the vapor pressure of pure liquid solute, and p_o the outlet pressure of the column. The second and third terms arise from the nonideality of the mobile gas phase with B_{ii} being the second virial coefficient of solute i and B_{ij} being the mixed virial coefficient of the solute with the carrier nitrogen gas (subscript j). The values of the virial coefficients (B_{ii} and B_{ij}) were obtained from the McGlashan and Potter[8] equation:

$$\frac{B_{ij}}{V_{ij}^c} = 0.430 - 0.886\left(\frac{T_{ij}^c}{T}\right) - 0.694\left(\frac{T_{ij}^c}{T}\right)^2 - 0.0375(n-1)\left(\frac{T_{ij}^c}{T}\right)^{4.5} \qquad (2)$$

Table 1. Vapor Pressures, Molar Volumes, and Virial Coefficients[5]

T / K	p_i^0 / kPa	V_i^0 / cm³·mol⁻¹	B_{ii} / cm³·mol⁻¹	B_{i2} / cm³·mol⁻¹	T / K	p_i^0 / kPa	V_i^0 / cm³·mol⁻¹	B_{ii} / cm³·mol⁻¹	B_{i2} / cm³·mol⁻¹
Pentane					1-Heptene				
308.15	97.7	118.13	−1073.84	46.73	308.15	11.98	143.85	−2627.23	60.84
318.15	136.09	120.22	−989.93	47.3	318.15	18.44	145.78	−2386.67	61.52
328.15	185.26	122.45	−916	47.84	328.15	27.5	147.8	−2178.27	62.15
Hexane					1-Octene				
308.15	30.63	132.95	−1732.27	53.48	308.15	3.94	159.35	−3534.92	62.84
318.15	45.05	134.95	−1584.52	54.11	318.15	6.42	161.28	−3190.86	63.55
328.15	64.46	137.05	−1455.62	54.7	328.15	10.07	163.29	−2894.48	64.21
Heptane					1-Hexyne				
308.15	9.84	148.57	−2623.49	59.69	308.15	27.21	114.51	−1630.99	49.15
318.15	15.32	150.55	−2382.53	60.37	318.15	40.47	116.15	−1490.57	49.77
328.15	23.09	152.62	−2173.85	61.01	328.15	58.5	117.88	−1368.18	50.35
Octane					1-Heptyne				
308.15	3.21	164.9	−3794.05	65.57	308.15	9.05	134.32	−2443.15	54.65
318.15	5.3	166.91	−3424.03	66.3	318.15	14.18	136.03	−2217.16	55.31
328.15	8.42	168.99	−3105.35	66.98	328.15	21.51	137.81	−2021.59	55.94
Cyclopentane					1-Octyne				
308.15	61.78	95.92	−1149.8	40.84	308.15	2.98	154.71	−3514.19	60.11
318.15	87.84	97.29	−1055.89	41.41	318.15	4.95	156.5	−3169.74	60.83
328.15	121.87	98.74	−973.61	41.95	328.15	7.92	158.36	−2873.23	61.49
Cyclohexane					Methanol				
308.15	20.08	110.16	−1853.02	45.81	308.15	27.95	40.16	−393.55	23.65
318.15	29.99	111.51	−1687.09	46.43	318.15	44.54	40.81	−368.2	24.08
328.15	43.52	112.92	−1543.08	47.02	328.15	68.75	41.49	−345.39	24.48
Cycloheptane					Ethanol				
308.15	4.79	119.82	−3047.04	49.84	308.15	13.52	59.92	−560.17	29.82
318.15	7.65	121.09	−2749.45	50.53	318.15	22.75	60.83	−524.08	30.31
328.15	11.79	122.4	−2493.23	51.17	328.15	36.88	61.79	−491.58	30.77
1-Hexene					Benzene				
308.15	37.21	127.79	−1607.05	51.63	308.15	20.31	90.63	−1631.98	40.36
318.15	54.19	129.73	−1470.51	52.23	318.15	30.55	91.72	−1484.56	40.95
328.15	76.82	131.77	−1351.33	52.8	328.15	44.61	92.85	−1356.71	41.49

Table 2. Critical Constants and Ionization Energies[5]

	V_c / cm³·mol⁻¹	T_c / K	I / kJ·mol⁻¹
pentane	304	469.7	998.6
hexane	370	507.5	977.4
heptane	432	540.3	957.1
octane	492	568.8	947.5
cyclopentane	260	511.6	1014.1
cyclohexane	308	553.5	951.3
cycloheptane	353	604.2	962
1-hexene	350	504	910.8
1-heptene	440	537.3	910.8
1-octene	464	566.7	909.9
1-hexyne	332	516.2	960
1-heptyne	387	547.2	960
1-octyne	442	574.2	951.3
methanol	118	512.6	1046.9
ethanol	167.1	513.9	1010.3
benzene	259	562.2	892.1
nitrogen	89.5	126.2	14.5

Here V^c and T^c are the critical volume and temperature, respectively. V_{12}^c and T_{12}^c were calculated from the critical properties of pure solute by using the combining rules.[9−11] The list of all the standard values is provided in Table 1. The critical constants are reported in Table 2.

The retention volume is expressed as

$$B_{ij} = JU_0(t_r - t_g)\frac{T_{col}}{T_F}\left[1 - \frac{p_{ow}}{p_o}\right] \quad (3)$$

Here U_0 is the flow rate of carrier gas, t_r is the retention time in seconds, and t_g is the dead time. The column temperature T_{col} and flow temperature T_f as well as the saturation pressure of water at flow temperature p_{ow} have to be provided. Methane is considered as a non-retainable component, so it was used to determine the dead time, and the retention time was adjusted accordingly. The adjusted retention time $t_r' = t_r - t_g$ was taken as the difference between the retention time of solute and dead time of methane. The dead time was measured everytime before a γ_i^∞ procedure was initiated. The factor J corrects the influence of pressure drop along the column which is given by

$$J = \frac{3}{2}\left(\frac{(p_i/p_o)^2 - 1}{(p_i/p_o)^3 - 1}\right) \quad (4)$$

Table 3. COSMO-RS Computational Details

steps used	computational details	ref
package used	Gaussian 03	23
gas-phase optimization	level of theory: PBV86/TZVP/DGA1	24
	basis set: TZVP	25
	density fitting basis set: DGA1	26
SCRF calculation	level of theory: PBV86/TZVP/DGA1	24
COSMO file generation	basis set: TZVP	25
	density fitting basis set: DGA1	26
radius of elements	Klamt et al.	12
radius of phosphorous	$1.17R_{Bondii}$	

Table 4. COSMO-RS Parameters Used in This Work

parameter	$\gamma\infty$ prediction (this work)
a_{eff}	6.32 Å²
α'	35191 (kJ·Å⁴)/(mol·e²)
c_{hb}	313525 (kJ·Å⁴)/(mol·e²)
σ_{hb}	0.0084 e·Å⁻²
r_{av}	0.81 Å

COSMO-RS Predictions

COSMO-RS is a novel a priori prediction method for thermodynamic equilibria of fluids and liquid mixtures. The details of this method can be found in some excellent papers of Klamt and co-workers.[12−14] In our earlier work, we have successfully predicted the vapor−liquid equilibria (VLE) of

Table 5. Average Infinite Dilution Activity Coefficients (γ_i^∞) Values for the Three Phosphonium ILs

	[thtd-Ph][Cl]			[thtd-Ph][BF4]			[thtd-Ph][(Tf)2N]		
solute	$T = 308.15$ K	$T = 318.15$ K	$T = 328.15$ K	$T = 308.15$ K	$T = 318.15$ K	$T = 328.15$ K	$T = 308.15$ K	$T = 318.15$ K	$T = 328.15$ K
Section A: Experimental Measurements									
pentane	0.607	0.599	0.594	0.722	0.706	0.695	0.611	0.602	0.597
hexane	0.766	0.753	0.746	0.968	0.942	0.925	0.766	0.751	0.742
heptane	0.816	0.803	0.795	1.000	0.970	0.952	0.783	0.769	0.761
octane	0.847	0.831	0.821	1.153	1.115	1.092	0.843	0.825	0.814
cyclopentane	0.579	0.576	0.574	0.638	0.630	0.625	0.562	0.559	0.558
cyclohexane	0.631	0.627	0.625	0.730	0.719	0.712	0.612	0.609	0.607
cycloheptane	0.861	0.753	0.763	1.000	0.979	0.965	0.787	0.779	0.774
1-hexene	0.477	0.471	0.468	0.570	0.558	0.551	0.501	0.494	0.490
1-heptene	0.523	0.515	0.511	0.663	0.647	0.637	0.558	0.549	0.543
1-octene	0.567	0.557	0.552	0.769	0.748	0.734	0.617	0.605	0.598
1-hexyne	0.449	0.461	0.468	0.345	0.358	0.366	0.454	0.463	0.468
1-heptyne	0.479	0.494	0.504	0.374	0.389	0.399	0.485	0.496	0.502
1-octyne	0.494	0.514	0.526	0.387	0.406	0.417	0.511	0.524	0.532
methanol	0.887	0.879	0.873	6.682	6.383	6.097	0.942	0.958	0.989
ethanol	0.740	0.737	0.735	5.593	5.361	5.138	0.884	0.894	0.902
benzene	0.408	0.403	0.400	0.370	0.367	0.366	0.406	0.403	0.402
Section B: COSMO-RS Predictions									
pentane	0.602	0.597	0.592	0.690	0.629	0.630	0.692	0.681	0.671
hexane	0.765	0.757	0.749	0.925	0.839	0.838	0.929	0.911	0.895
heptane	0.758	0.749	0.741	0.956	0.864	0.863	0.954	0.935	0.917
octane	0.837	0.826	0.816	1.102	0.993	0.989	1.102	1.077	1.053
cyclopentane	0.557	0.556	0.555	0.610	0.561	0.566	0.630	0.625	0.620
cyclohexane	0.609	0.607	0.605	0.698	0.641	0.645	0.717	0.710	0.703
cycloheptane	0.779	0.774	0.769	0.956	0.872	0.874	0.982	0.967	0.953
1-hexene	0.502	0.497	0.494	0.545	0.497	0.499	0.553	0.545	0.538
1-heptene	0.558	0.553	0.547	0.634	0.576	0.577	0.638	0.627	0.617
1-octene	0.619	0.612	0.605	0.735	0.666	0.665	0.735	0.721	0.708
1-hexyne	0.307	0.319	0.330	0.330	0.319	0.332	0.328	0.338	0.348
1-heptyne	0.321	0.334	0.347	0.358	0.347	0.361	0.358	0.371	0.382
1-octyne	0.351	0.365	0.379	0.370	0.362	0.378	0.406	0.419	0.432
methanol	0.887	0.879	0.873	6.388	5.687	5.524	1.136	1.153	1.187
ethanol	0.740	0.737	0.735	5.347	4.777	4.655	1.061	1.073	1.082
benzene	0.370	0.371	0.372	0.354	0.327	0.332	0.373	0.372	0.371

ILs.[15] Diedenhofen et al.[16] has predicted the γ^∞ values for imidazolium-based ILs. The details of COSMO-RS and related equations and the COSMO files used are given in our previous paper.[15] The computational details are given in Table 3.

The various interaction energy terms are as follows: the misfit e_{misfit}, the hydrogen bonding e_{hb}, and the van der Waals e_{vdW}. The misfit of the partners arises when $\sigma + \sigma'$ does not vanish where σ and σ' are the screening charge densities in e·Å^{-2} of the interacting segment pair. The hydrogen-bonding term e_{hb} comes into play only if two sufficiently polar pieces of surface of opposite polarity are in contact and becomes important with increasing polarity. The van der Waals (vdW) energy contribution is expressed by element-specific dispersion coefficient parameters (e), which have to be fitted to experimental data. The vdW energy gained by a molecule X during the transfer from the gas phase to any liquid phase is not an interaction term but a state of the molecule embedded with vdW interacting surface species.

The interactions of molecular surfaces in COSMO-RS are given by an interaction energy functional $e(\sigma, \sigma') = e_{misfit}(\sigma, \sigma') + e_{hb}(\sigma, \sigma')$ and depends only on the screening charge densities. The vdW contribution is subsumed in the reference state energy. The generic interaction functional $e(\sigma, \sigma')$ has three adjustable parameters (α', σ_{hb}, and c_{hb}) that are obtained using a simultaneous scheme and are used from our recent work on liquid−liquid equilibria.[17] The values are given in Table 4. In addition to these explicit parameters, the screening charge densities also depend on the element-specific radii that are used in the cavity construction and roughly fixed by the rule 1.17 R_{Bondi}. Thus there are three general parameters plus two element-specific parameters per element. For the nine elements H, C, N, O, F, S, Cl, Br, and I, we have altogether 21 parameters.

If the liquid system under consideration is a pure liquid X, then the σ-profile $p_S(\sigma)$ of the system is identical with the σ-profile $p^X(\sigma)$ of the pure compound. In general, a system may be a mixture consisting of several compounds X with molar concentrations x_i. The screening charge densities from the COSMO output are averaged with an averaging radius ($r_{av} = 0.81$ Å) to give the "apparent" charge density σ_m on a surface segment. The σ-profile of the system is given by the weighted sum of the σ-profiles of the components. An exact expression for the σ potential of these segments is based on rigorous statistical mechanical arguments.[14] Then the activity coefficient of segment in the mixture and in the pure liquid, $\Gamma_S(\sigma)$ and $\Gamma_i(\sigma)$, and subsequently activity coefficient of each component is computed. Molecular volumes and areas from COSMO calculation are normalized by a standard volume (66.69 Å^3) and surface area (79.53 Å^2) to yield the r and q parameters that are used for computing the Staverman−Guggenheim term.

Results and Discussion

Table 5, Section A, lists the experimental γ_i^∞ values at $T =$ (308.15, 318.15, and 328.15) K for the three ILs. In the three ILs, the activity coefficients for all the solutes apart from alcohols are below unity, indicating a strong affinity of the solutes for the IL stationary phase. The values are 1 order of magnitude less when compared with the pyridinium-[18] or imidazolium-[19,20] based ILs. In pyridinium or imidazolium ILs, the cation is surrounded by relatively short chained alkyl groups (methyl to octyl). The charge delocalization due to such imidazolium rings is better as compared to the phosphonium IL where delocalization is nonexistent due to a bulky central quaternary inorganic cation. The relative strength of Coulombic attractive forces decreases due to the bulky nature of the cation.

Table 6. Straight Line Fit of γ^{∞} as a Function of Carbon Number (eq 5)

	[thtd-Ph][Cl]			[thtd-Ph][BF4]			[thtd-Ph][(Tf)2N]		
	A	*B*	SD[a]	*A*	*B*	SD[a]	*A*	*B*	SD[a]
				$T = 308.15$ K					
alkanes	0.077	0.258	0.092	0.181	−0.296	0.155	0.112	−0.021	0.086
cycloalkanes	0.141	−0.155	0.032	0.145	0.049	0.070	0.071	−0.287	0.041
alkenes	0.022	0.339	0.106	0.021	0.242	0.133	0.028	0.312	0.084
alkynes	0.045	0.252	0.016	0.099	0.070	0.015	0.058	0.210	0.020
				$T = 318.15$ K					
alkanes	0.075	0.260	0.147	0.174	−0.271	0.147	0.110	−0.110	0.082
cycloalkanes	0.088	0.121	0.067	0.091	0.313	0.067	0.068	0.291	0.039
alkenes	0.043	0.213	0.128	0.024	0.240	0.128	0.03	0.311	0.082
alkynes	0.026	0.304	0.017	0.095	0.081	0.017	0.055	0.216	0.022
				$T = 328.15$ K					
alkanes	0.094	0.087	0.088	0.170	−0.250	0.142	0.108	−0.001	0.080
cycloalkanes	0.073	0.264	0.030	0.121	0.124	0.065	0.067	0.293	0.038
alkenes	0.029	0.325	0.103	0.025	0.241	0.125	0.032	0.308	0.080
alkynes	0.042	0.258	0.021	0.091	0.092	0.018	0.054	0.219	0.023

[a] SD, standard deviation.

Phosphonium ILs may be expected to be hydrophobic in nature with a fairly open structure for the retention of hydrocarbon solutes. The activity coefficients of all the solutes in general increases linearly with carbon atom. Cyclization of the alkane skeleton (e.g., cyclohexane) reduces the value in comparison to the corresponding linear alkanes (e.g., hexane). The infinite dilution activity coefficients can be extrapolated as a function of the number of carbon atoms. Thus for a homologous series, the following straight line equation will hold:

$$\gamma_i^{\infty} = An + B \tag{5}$$

where *A* and *B* are constants and *n* is the number of carbon atoms. The constants *A* and *B* along with the standard deviations are given in Table 6. The standard deviations are found to be higher for alkanes and alkenes, being in the range (0.10 to 0.15). In general the γ^{∞} values follow the following pattern:

alkanes > cycloalkanes > alkenes > alkynes > benzene

The variation of the γ^{∞} values with carbon number for [thtd-Ph][Cl] is shown in Figure 2. It is interesting to compare the results previously reported for the IL [thtd-Ph][$(C_2F_5)_3PF_3$].[5] The γ_i^{∞} values in general distinctly lower in this ∞ IL even though the general dependence on chain length and branching shows

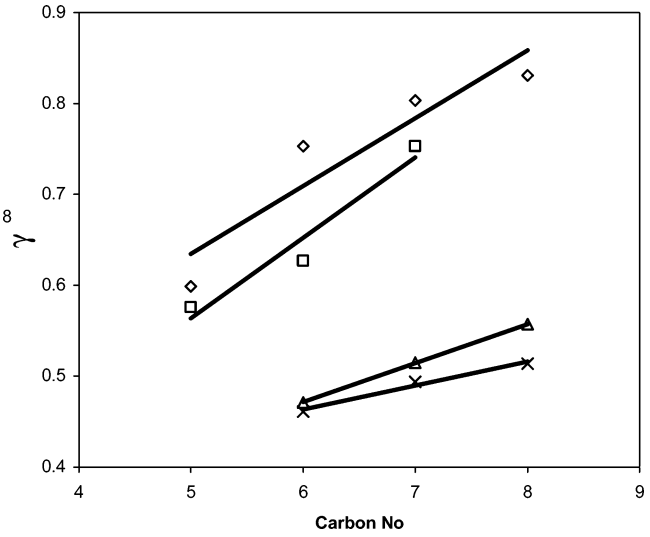

Figure 2. Variation of experimental γ_i^{∞} with carbon number in [thtd-Ph][Cl]: ◇, alkanes; □, cycloalkanes; △, alkenes; ×, alkynes at $T = 318.15$ K.

Table 7. COSMO-RS γ_i^{∞} Values for Alcohols at $T = 298.15$ K

	[thtd-Ph][Cl]	[thtd-Ph][BF4]	[thtd-Ph][(Tf)2N]
methanol	0.887	6.388	1.136
ethanol	0.740	5.347	1.061
1-propanol	0.604	4.530	0.141
butanol	0.099	0.758	0.041
pentanol	0.096	0.766	0.042
hexanol	0.063	0.445	0.033
heptanol	0.047	0.377	0.024

Table 8. Molar Excess Enthalpy at Infinite Dilution

	$H_i^{E,\infty}$/J·mol^{-1}		
compound	[thtd-Ph][Cl]	[thtd-Ph][BF4]	[thtd-Ph][(Tf)2N]
pentane	96 ± 4.6	115 ± 4.4	125 ± 4.8
hexane	142 ± 5.4	170 ± 6.5	185 ± 7.0
heptane	138 ± 5.2	166 ± 6.3	179 ± 6.8
octane	216 ± 8.2	259 ± 9.8	281 ± 10.7
cyclopentane	79 ± 1.6	95 ± 1.9	103 ± 2.1
cyclohexane	231 ± 4.6	277 ± 5.5	300 ± 6.0
cycloheptane	273 ± 5.5	328 ± 6.6	355 ± 7.1
1-hexene	78 ± 2.7	94 ± 3.2	101 ± 3.4
1-heptene	85 ± 2.9	102 ± 3.5	111 ± 3.8
1-octene	127 ± 4.3	152 ± 5.2	165 ± 5.6
1-hexyne	60 ± 2.5	72 ± 3.0	78 ± 3.3
1-heptyne	72 ± 10.7	86 ± 12.8	94 ± 13.9
1-octyne	306 ± 17.1	367 ± 20.5	398 ± 22.2
methanol	488 ± 19.5	586 ± 23.4	634 ± 25.4
ethanol	616 ± 24.6	739 ± 29.6	801 ± 32.0
benzene	84 ± 4.2	101 ± 5.1	109 ± 5.5

the same trends as in the case with the three ILs studied in the present work. The IL [thtd-Ph][BF_4] owing to its smaller size of its BF_4 anion gives rise to a stronger Coulombic interaction. Dissolution of a neutral molecule in this IL requires more interaction energy to be broken than in the case of the ILs with the larger bis(trifluoromethyl-sulfonyl) imide ion $(Tf)_2N$. It was observed that the values of γ^{∞} decreases with increasing chain length. In order to have an insight, the values for propanol, butanol, pentanol, hexanol, and heptanol have been derived using COSMO-RS predictions at $T = 298.15$ K. The γ_i^{∞} values tend to decrease with increasing chain length of alcohols (Table 7).

The value for the partial molar excess enthalpy at infinite dilution $H_i^{E,\infty}$ can be directly obtained from the slope of a straight line derived from

$$\left(\frac{\partial \ln \gamma_{i3}^{\infty}}{\partial (1/T)}\right) = -\frac{H_i^{E,\infty}}{R} \tag{6}$$

where *R* is the gas constant. The values of $H_i^{E,\infty}$ with their

Table 9. Selectivities (S_{ij}^{∞}) at Infinite Dilution of Various Ionic Liquids

ionic liquid	ref	T/K	hexane/ benzene	cyclohexane/ benzene	hexene/ benzene	methanol/ benzene	ethanol/ benzene
[BMIM][$(Tf)_2N$]	18	298.15	17.50	8.72	10.59	1.47	2.14
[HMIM][BF_4]	19	298.15	19.47	11.06	8.62	0.80	
[HMIM][PF_6]	20	298.15	18.46	10.19	8.74	1.88	
[1,2-EMIM] [$(Tf)_2N$]	21	313.15	22.98			1.33	1.86
[OMIM][BF_4]	27	298.15	10.42	6.77	5.93	0.89	1.47
[$(CH_3)_3BA$][$(Tf)_2N$][a]	28	298.15	14.49	4.20	7.74	1.22	1.67
[BMIM][MeEt-SO_4][b]	29	298.15	35.03	15.47	2.42	0.17	
[BMIM][$OcSO_4$][c]	30	313.15	5.27	4.00	1.66	0.26	
[EMIM] [$(Tf)_2N$]	31	313.15	21.53			0.97	1.15
[PY][$EthSO_4$][d]	32	298.15	11.86	5.17	9.58		
[EPy] [$(Tf)_2N$][e]	32	313.15	24.39	13.23	10.46	0.94	1.32
[HMIM] [$(Tf)_2N$]	33	298.15	12.36	7.03	2.79	1.70	2.70
[thtd-Ph][$(C_2F_5)_3PF_3$]	5	308.15	3.30	2.50	2.79	6.15	6.0
[thtd-Ph][Cl]	this work	308.15	1.99	1.28	0.70	2.17	1.81
[thtd-Ph][BF_4]	this work	308.15	2.62	1.79	1.73	18.0	14.6
[thtd-Ph] [$(Tf)_2N$]	this work	308.15	1.89	1.37	1.38	2.52	2.37

[a] Trimethylbutylammonium bis(trifluoromethylsulfonyl) imide. [b] 1-Butyl-3-methylimidazolium 2-(2-methoxyethoxy)ethyl sulfate. [c] 1-Butyl-3-methylimidazolium octyl sulfate. [d] Pyridinium ethoxysulfate. [e] *N*-Ethylpyridinium bis(trifluoromethylsulfonyl)imide.

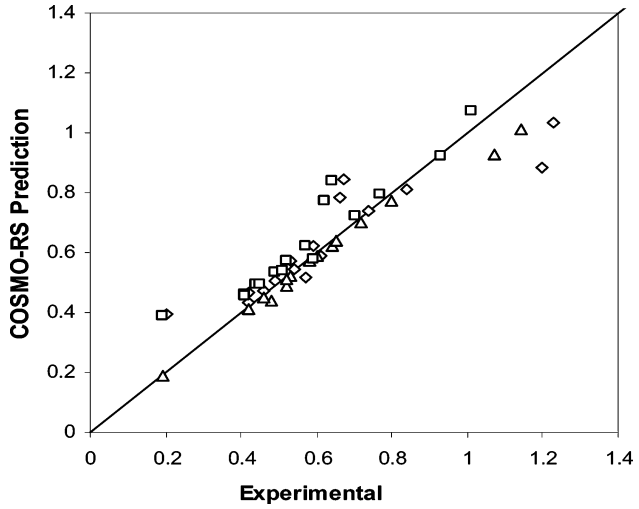

Figure 3. Benchmarking COSMO-RS predictions with [thtd-Ph][$(C_2F_5)_3PF_3$]: ◇, 308.15 K; △, 318.15 K; □, 328.15 K.

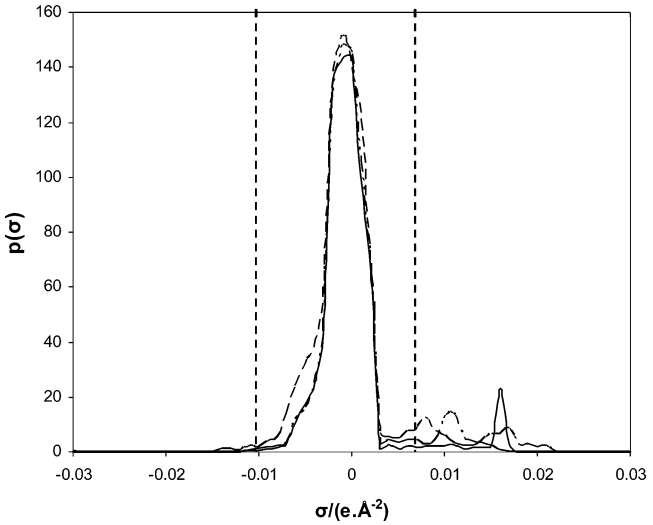

Figure 4. σ profiles for the phosphonium ILs studied in this work. —, [thtd-Ph][Cl]; - - -, [thtd-Ph][BF_4]; — —, [thtd-Ph][$(Tf)_2N$]. The dotted line in the figure shows the cutoff zone for hydrogen bonding.

uncertainties for the compounds studied are also listed in Table 8. The results are similar for the three phosphonium-based ILs. All the values are seen to be positive. $H_i^{E,\infty}$ values are positive and increase with increasing chain length of the linear alkanes. The introduction of double bonds decrease the positive values of $H_i^{E,\infty}$. To date, no direct calorimetric measurements are available for phosphonium ILs so a comparison with the exact data could not be made. The overall uncertainty obtained was ± 5 %, which is close to the values obtained by Heintz et al.[21]

To effectively define the separation power of the solvent, the selectivity of the ILs are calculated. The selectivity was defined by the following relation:

$$S_{ij} = \frac{\gamma_i^{\infty}}{\gamma_j^{\infty}} \tag{7}$$

where *i* and *j* represent two components to be separated by the IL solvent. The selectivities at infinite dilution have been calculated using eq 7 and then compared with the reported selectivities in Table 9. The values are 1 order of magnitude less than that of imidazolium-, pyridinium-, and ammonium-based ILs. Most of the selectivities values are quite less and closer to unity, indicating the poor separation of the phosphonium ILs. The selectivities as given in Table 8 have a significance as the values for alcohol−aromatic separation using [thtd-Ph][BF_4] are the highest when compared with imidazolium or pyridinium ILs. The selectivities ($\gamma_i^{\infty} = 14.95$ for benzene−ethanol and 18.6 for benzene−methanol) are comparable to that obtained for benzene−hexane separation for [HMIM][PF_6] (18.46), [HMIM][BF_4] (19.47), and [BMIM][$(Tf)_2N$] (17.50). Although the separation of aromatics and alcohols is not well-reported in literature, the selectivity values obtained with [thtd-Ph][BF_4] are the highest among all the ILs.

However, the selectivity values in other ILs ([thtd-Ph][$(Tf)_2N$] and [thtd-Ph][Cl]) are low. For both methanol−benzene and ethanol−benzene separation the selectivities increases with temperature for the ILs: [thtd-Ph][$(Tf)_2N$] and [thtd-Ph][Cl]. But for [thtd-Ph][BF_4], it is the reverse.

COSMO-RS Benchmarking. In this work, we will first test our prediction on the experimental data of the IL [thtd-Ph][$(C_2F_5)_3PF_3$].[5] The reported and predicted data are shown in Figure 3. The average absolute deviation is 11.5 % for all the temperatures taken together. The absolute average deviation is calculated from the following equation:

$$\mathrm{AAD} = \frac{1}{N}\sum_{i=1}^{N}\left(\frac{\gamma_{i,\mathrm{expt}}^{\infty} - \gamma_{i,\mathrm{calc}}^{\infty}}{\gamma_{i,\mathrm{expt}}^{\infty}}\right) \tag{8}$$

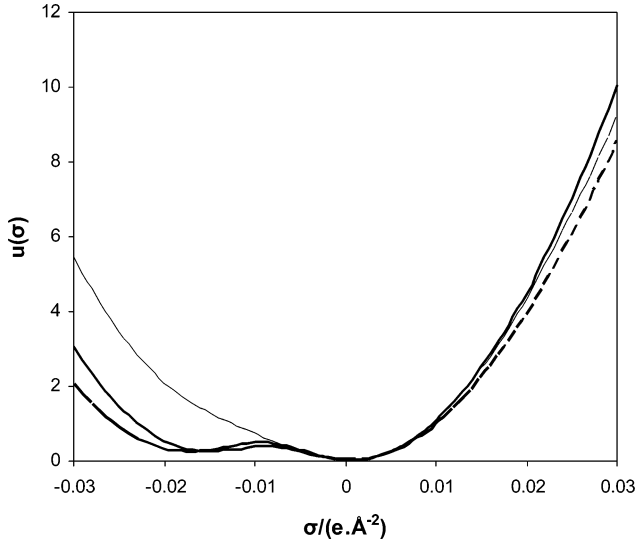

Figure 5. σ potentials for the phosphonium ILs studied in this work. —, [thtd-Ph][Cl]; - - -, [thtd-Ph][BF_4]; — —, [thtd-Ph][$(Tf)_2N$].

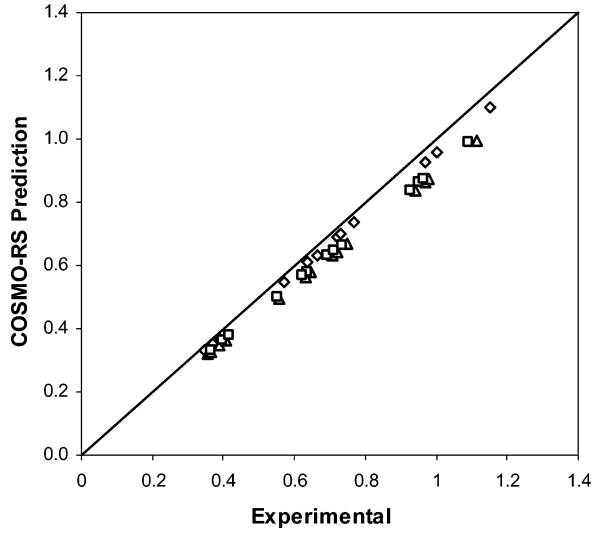

Figure 6. Comparison and prediction of γ_i^∞ for [thtd-Ph][BF_4]: ◇, 308.15 K; △, 318.15 K; □, 328.15 K.

Here N is the number of compounds in a particular IL. The predictions for most of the compounds are in good agreement except for benzene and ethanol.

σ Profiles and Potentials. The σ profiles for all the three phosphonium ILs have been shown in Figure 4. Looking at the profiles, all the three ILs are nonpolar in nature as greater part of their peaks lie between the range: $\sigma = -0.0084$ e·Å^{-2} and $\sigma = 0.0084$ e·Å^{-2}, which is the cutoff surface charge density for hydrogen bonding. This proves our earlier point that the nonpolarity is attained primarily due to the inefficient delocalization of the charge. The phosphonium cation has a greater peak area as compared to the anion. It should be noted that the anion causes positive screening charge densities and thus show up in the positive region of the curve and for the cation it is the vice versa. The two vertical dashed lines are the locations of the cutoff values for the hydrogen bond donor($\sigma_{hb} < -0.0084$ e·Å^{-2}) and acceptor for $\sigma_{hb} > 0.0084$ e·Å^{-2}.

There is a competing effect between the free energy of removing the screening charges(positive) and that of forming hydrogen bonds (negative). Thus if a strong hydrogen bond is formed, the net restoring free energy ($\mu(\sigma)$) is negative. In the σ potentials (Figure 5), all the three potentials are similar. The absence of any screening charge densities outside the cutoff zone made the net restoring free energies positive, thus contributing no hydrogen bonding.

Testing Systems. After benchmarking COSMO-RS predictions have been obtained for the three ILs. The predictions for the IL [thtd-Ph][BF_4] is shown in Figure 6. The COSMO-RS predictions for all the ILs have been given in Table 5, Section B. The predictions for all the three ILs match closely with experimental values. The overall absolute average deviations for [thtd-Ph][Cl], [thtd-Ph][BF_4], and [thtd-Ph][$(Tf)_2N$] are 9 %, 8 %, and 16 %, respectively.

Conclusions

Phosphonium-based ILs are poor solvents for separation processes of aliphatic and aromatic as seen in the case of benzene−hexane, benzene−hexane, benzene−alcohol, and benzene−cyclohexane separation. However the IL [thtd-Ph][BF_4] has moderate selectivity for benzene−alcohol mixtures. The predictive schemes of COSMO-RS have confirmed our experimental results and proved that the phosphonium ILs are nonpolar in nature as seen from its σ profile.

Acknowledgment

We are grateful to Chromatopak Analytical Inc.[22] (Mumbai, India) for fabricating the column and coating it with the stationary liquid phase (IL). The authors also thank Rahul Kumar (final year student of IIT, Roorkee, India) for helping out in the experimental work.

Supporting Information Available:

Appendix I gives the COSMO files for four phosphonium ILs generated by Gaussian 03.[23] This material is available free of charge via the Internet at http://pubs.acs.org.

Literature Cited

(1) Brennecke, J. F.; Maginn, E. J. Ionic liquids: innovative fluids for chemical processing. *AIChE J.* **2001**, *47*, 2384−2389.
(2) Marsh, N. K.; Boxall, A. J.; Lichtenthaler, R. Room temperature ionic liquids and their mixtures—a review. *Fluid Phase Equilib.* **2004**, *219*, 93−98.
(3) Heintz, A. Recent developments in thermodynamics and thermophysics of non -aqueous mixtures containing ionic liquids. A review. *J. Chem. Thermodyn.* **2005**, *37*, 525−535.
(4) Esperanca, J. M. S. S.; Guedes, H. J. R.; Blesic, M.; Rebelo, L. P. N. Densities and derived thermodynamic properties of ionic liquids. 3. Phosphonium-based ionic liquids over an extended pressure range. *J. Chem. Eng. Data* **2006**, *51*, 237−242.
(5) Letcher, T. M.; Reddy, P. Determination of activity coefficients at infinite dilution of organic solutes in the ionic liquid, trihexyl-(tetradecyl)phosphonium tris(pentafluoroethyl) trifluorophosphate, by gas−liquid chromatography. *Fluid Phase Equilib.* **2005**, *235*, 11−17.
(6) Letcher, T. M.; Soko, B.; Reddy, P.; Deenadayalu, N. Determination of activity coefficients at infinite dilution of solutes in the ionic liquid 1-hexyl-3-methylimidazolium tetrafluoroborate using gas−liquid chromatography at the temperatures 298.15 K and 323.15 K. *J. Chem. Eng. Data* **2003**, *48*, 1587−1590.
(7) Cruickshank, A. J. B.; Gainey, B. W.; Hicks, C. P.; Letcher, T. M.; Moody, R. W.; Young, C. L. Gas−liquid chromatographic determination of cross-term second virial coefficients using glycerol. *Trans. Faraday Soc.* **1969**, *65*, 1014−1031.
(8) McGlashan, M. L.; Potter, D. J. B. An apparatus for the measurement of the second viral coefficients of vapours; the second viral coefficients of some *n*-alkanes and of some mixtures of *n*-alkanes. *Proc. R. Soc.* **1962**, *267*, 478−500.
(9) Young, C. L.; Conder, J. R. *Physicochemical Measurements by Gas Chromatography*; Wiley: New York, 1979.
(10) Hudson, G. H.; McCoubrey, J. C. Intermolecular forces between unlike molecules. *Trans Faraday Soc.* **1960**, *56*, 761−771.
(11) Cruickshank, A. J. B.; Windsor, M. L.; Young, C. L. Prediction of second virial coefficients of mixtures from the principle of corresponding states. *Trans. Faraday Soc.* **1966**, *62*, 23341−23355.
(12) Klamt, A. Conductor like screening model for real solvents: a new approach to the quantitative calculation of solvation phenomena. *J. Phys. Chem.* **1995**, *99*, 2224−2235.

(13) Klamt, A. *COSMO-RS: From Quantum Chemistry to Fluid Phase Thermodynamics and Drug Design*, 1st ed.; Elsevier: Amsterdam, 2005.
(14) Klamt, A.; Jonas, V.; Buerger, T.; Lohrenz, J. C. W. Refinement and parameterization of COSMO-RS. *J. Phys. Chem. A* **1998**, *102*, 5074−5085.
(15) Banerjee, T.; Singh, M. K.; Khanna, A. Prediction of binary VLE for imidazolium based ionic liquid systems using COSMO-RS. *Ind. Eng. Chem. Res.* **2006**, *45*, 3207−3219.
(16) Diedenhofen, M.; Eckert, F.; Klamt, A. Prediction of infinite dilution activity coefficients of organic compounds in ionic liquids using COSMO-RS. *J. Chem. Eng. Data* **2003**, *48*, 475−479.
(17) Banerjee, T.; Sahoo, R. K.; Khanna, A. Multi-component liquid−liquid equilibria prediction for aromatic extraction systems using COSMO-RS. *Ind. Eng. Chem. Res.* (submitted for publication).
(18) Heintz, A.; Casás, M. L.; Nesterov, A. I.; Emel'yanenko, N. V.; Verevkin, S. P. Thermodynamic properties of mixtures containing ionic liquids. 5. Activity coefficients at infinite dilution of hydrocarbons, alcohols, esters, and aldehydes in 1-methyl-3-butylimidazolium bis-(trifluoromethylsulfonyl) imide using gas−liquid chromatography. *J. Chem. Eng. Data* **2005**, *50*, 1510−1514.
(19) Letcher, T. M.; Soko, B.; Reddy, P.; Deenadayalu, N. Determination of activity coefficients at infinite dilution of solutes in the ionic liquid 1-hexyl-3-methylimidazolium tetrafluoroborate using gas−liquid chromatography at the temperatures 298.15 K and 323.15 K. *J. Chem. Eng. Data* **2003**, *48*, 1587−1590.
(20) Letcher, T. M.; Soko, B.; Ramjugernath, D.; Deenadayalu, N.; Nevines, A.; Naicker, P. K. Activity coefficients at infinite dilution of organic solutes in 1-hexyl-3-methylimidazolium hexafluorophosphate from gas−liquid chromatography. *J. Chem. Eng. Data* **2003**, *48*, 708−711.
(21) Heintz, A.; Kulikov, D. V.; Verevkin, S. P. Thermodynamic properties of mixtures containing ionic liquids. 2. Activity coefficients at infinite dilution of hydrocarbons and polar solutes in 1-methyl-3-ethylimidazolium bis(trifluoromethyl-sulfonyl) amide and in 1,2-dimethyl-3-ethylimidazolium Bis(trifluoromethyl-sulfonyl) amide using gas−liquid chromatography. *J. Chem. Eng. Data* **2002**, *47*, 894−899.
(22) Chromatopak Analytical Private Limited, Mumbai, India (www.chromatopak.com).
(23) Frisch, M. J.; Trucks, G. W.; Schlegel, H. B.; Scuseria, G. E.; Robb, M. A.; Cheeseman, J. R.; Zakrzewski, V. G.; Montgomery, J. A., Jr.; Stratmann, R. E.; Burant, J. C.; Dapprich, S.; Millam, J. M.; Daniels, A. D.; Kudin, K. N.; Strain, M. C.; Farkas, O.; Tomasi, J.; Barone, V.; Cossi, M.; Cammi, R.; Mennucci, B.; Pomelli, C.; Adamo, C.; Clifford, S.; Ochterski, J.; Petersson, G. A.; Ayala, P. Y.; Cui, Q.; Morokuma, K.; Salvador, P.; Dannenberg, J. J.; Malick, D. K.; Rabuck, A. D.; Raghavachari, K.; Foresman, J. B.; Cioslowski, J.; Ortiz, J. V.; Baboul, A. G.; Stefanov, B. B.; Liu, G.; Liashenko, A.; Piskorz, P.; Komaromi, I.; Gomperts, R.; Martin, R. L.; Fox, D. J.; Keith, T.; Al-Laham, M. A.; Peng, C. Y.; Nanayakkara, A.; Challacombe, M.; Gill, P. M. W.; Johnson, B.; Chen, W.; Wong, M. W.; Andres, J. L.; Gonzalez, C.; Head-Gordon, M.; Replogle, E. S.; Pople, J. A. *Gaussian 03*, *Revision B.05*; Gaussian, Inc.: Pittsburgh, PA, 2003.
(24) Perdew, J. P. Density-functional approximation for the correlation energy of the inhomogeneous electron gas. *Phys. Rev. B* **1986**, *33*, 8822−8824.
(25) Schäfer, A.; Huber, C.; Ahlrichs, R. Fully optimized contracted Gaussian basis sets of triple zeta valence quality for atoms Li to Kr. *J. Chem. Phys.* **1994**, *100*, 5829−5835.
(26) Sosa, C.; Andzelm, J.; Elkin, B. C.; Wimmer, E.; Dobbs, K. D.; Dixon, D. A. A local density functional study of the structure and vibrational frequencies of molecular transition-metal compounds. *J. Phys. Chem.* **1992**, *96*, 6630−6636.
(27) Heintz, A.; Verevkin, S. P. Thermodynamic properties of mixtures containing ionic liquids. 6. Activity coefficients at infinite dilution of hydrocarbons, alcohols, esters, and aldehydes in 1-methyl-3-octylimidazolium tetrafluoroborate using gas−liquid chromatography. *J. Chem. Eng. Data* **2005**, *50*, 1515−1519.
(28) Heintz, A.; Vasiltsova, T. V.; Safarov, J.; Bich, E.; Verevkin, S. P. Thermodynamic properties of mixtures containing ionic liquids. 9. Activity coefficients at infinite dilution of hydrocarbons, alcohols, esters, and aldehydes in trimethyl-butylammonium bis(trifluoromethylsulfonyl) imide using gas−liquid chromatography and static method. *J. Chem. Eng. Data* **2006**, *51*, 648−655.
(29) Letcher, T. M.; Domanska, U.; Marciniak, M.; Marciniak, A. Activity coefficients at infinite dilution measurements for organic solutes in the ionic liquid 1-butyl-3-methyl-imidazolium 2-(2-methoxyethoxy) ethyl sulfate using g.l.c. at T = (298.15, 303.15, and 308.15) K. *J. Chem. Thermodyn.* **2005**, *37*, 587−593.
(30) Letcher, T. M.; Domanska, U.; Marciniak, M.; Marciniak, A. Determination of activity coefficients at infinite dilution of solutes in the ionic liquid 1-butyl-3-methylimidazolium octyl sulfate using gas−liquid chromatography at a temperature of 298.15 K, 313.15 K, or 328.15 K. *J. Chem. Eng. Data* **2005**, *50*, 1294−1298.
(31) Deenadayalu, N.; Letcher, T. M.; Reddy, P. Determination of activity coefficients at infinite dilution of polar and nonpolar solutes in the ionic liquid 1-ethyl-3-methyl-imidazolium bis(trifluoromethylsulfonyl) imidate using gas−liquid chromatography at the temperature 303.15 K or 318.15 K. *J. Chem. Eng. Data* **2005**, *50*, 105−108.
(32) Kato, R.; Gmehling, J. Activity coefficients at infinite dilution of various solutes in the ionic liquids $[MMIM]^+$ $[CH_3SO_4]^-$, $[MMIM]^+$ $[CH_3OC_2H_4SO_4]^-$, $[MMIM]^+[(CH_3)_2PO_4]^-$ $[C_5H_5NC_2H_5]^+[(CF_3SO_2)_2N]^-$ and $[C_5H_5NH]^+[C_2H_5OC_2H_4OSO_3]^-$. *Fluid Phase Equilib.* **2004**, *226*, 37−44.
(33) Letcher, T. M.; Marciniak, A.; Marciniak, M.; Domanska, U. Activity coefficients at infinite dilution measurements for organic solutes in the ionic liquid 1-hexyl-3-methylimidazolium bis(trifluoromethylsulfonyl)-imide using g.l.c. at T = (298.15, 313.15, and 333.15) K. *J. Chem. Thermodyn.* **2005**, *37*, 1327−1331.

Received for review June 26, 2006. Accepted August 27, 2006.

JE0602925